THE ASTROPHYSICAL JOURNAL, 425:122–126, 1994 April 10


# INITIAL MASS FUNCTIONS FROM ULTRAVIOLET STELLAR PHOTOMETRY: A COMPARISON OF LUCKE AND HODGE OB ASSOCIATIONS NEAR 30 DORADUS WITH THE NEARBY FIELD

JESSE K. HILL,[1] JOAN E. ISENSEE,[1] ROBERT H. CORNETT,[1] RALPH C. BOHLIN,[2] ROBERT W. O'CONNELL,[3] MORTON S. ROBERTS,[4] ANDREW M. SMITH,[5] AND THEODORE P. STECHER[5]

*Received 1993 September 2; accepted 1993 October 12*

## ABSTRACT

UV stellar photometry is presented for 1563 stars within a 40′ circular field in the LMC, excluding the 10′ × 10′ field centered on R136 investigated earlier by Hill et al. (1993). Magnitudes are computed from images obtained by the Ultraviolet Imaging Telescope in bands centered at 1615 Å and 2558 Å. Stellar masses and extinctions are estimated for the stars in associations using the evolutionary models of Schaerer et al. (1993), assuming the age is 4 Myr and that the local LMC extinction follows the Fitzpatrick (1985) 30 Dor extinction curve. The estimated slope of the initial mass function (IMF) for massive stars ($>15\ M_\odot$) within the Lucke and Hodge (LH) associations is $\Gamma = -1.08 \pm 0.2$. Initial masses and extinctions for stars not within LH associations are estimated assuming that the stellar age is either 4 Myr or half the stellar lifetime, whichever is larger. The estimated slope of the IMF for massive stars not within LH associations is $\Gamma = -1.74 \pm 0.3$ (assuming continuous star formation), compared with $\Gamma = -1.35$, and $\Gamma = -1.7 \pm 0.5$, obtained for the Galaxy by Salpeter (1955) and Scalo (1986), respectively, and $\Gamma = -1.6$ obtained for massive stars in the Galaxy by Garmany, Conti, & Chiosi (1982). The shallower slope of the association IMF suggests that not only is the star formation rate higher in associations, but that the local conditions favor the formation of higher mass stars there. We make no corrections for binaries or incompleteness.

*Subject headings:* Magellanic Clouds — open clusters and associations: individual (30 Doradus) — stars: luminosity function, mass function — ultraviolet: stars

## 1. INTRODUCTION

Star formation is now, or has recently been, occurring over the entire 30 Dor region of the LMC. This region has been the subject of several recent photometric investigations using ground-based optical images (Parker 1992; Schild & Testor 1992), WFPC optical images obtained by *HST* (Heap, Ebbets, & Malamuth 1993; Malamuth & Heap 1993; Campbell et al. 1992), and ultraviolet images obtained by the Ultraviolet Imaging Telescope (UIT) during the 1990 Astro-1 spacelab mission (Cheng et al. 1992; Hill et al. 1993). The OB associations LH 89, LH 90, LH 97, LH 99, LH 104, and LH 111, identified by Lucke & Hodge (1970), are entirely or partially contained within a 40′ diameter circular field imaged by UIT. In this investigation, stellar photometry for 1563 stars is obtained from images in the UIT bands B5 (wavelength centroid 1615 Å) and A5 (wavelength centroid 2558 Å). The photometry is described in § 2.

Stellar initial masses are estimated using the UV magnitudes together with evolutionary models and model atmospheres in § 3. Local LMC extinctions, assumed to follow the 30 Dor extinction curve of Fitzpatrick (1985), are determined simultaneously with the masses. We estimate the initial mass function (IMF) for massive stars ($>15\ M_\odot$) in the associations and for massive field stars not in associations in § 4. UV observations of an LMC field containing stars in associations, as well as field stars, are ideal for investigating the massive star IMF, since the distance to the stars is known and the stars are bright.

Table 1 lists the UIT images used in this investigation, giving the filter and the exposure time in seconds. UIT film images are reduced to flux-calibrated arrays of integers, as described in Stecher et al. (1992). Astrometric solutions are derived for the images using *Space Telescope* guide stars as astrometric standards (Lasker et al. 1990).

Figure 1*a* (Plate 8) shows UIT image NUV0128, the 472 s A5 (2558 Å) exposure, resampled to a north-up, east-left orientation. The Lucke & Hodge (1970) associations are outlined and labeled. Figure 1*b* (Plate 9) shows the same field from the 473 s B5 exposure FUV0137.

## 2. PHOTOMETRY

IDL implementations of DAOPHOT (Stetson 1987) algorithms are used to locate stars and perform aperture and PSF-fit photometry. Aperture photometry uses an aperture of radius 3.″4 (3 pixels). PSF-fit photometry uses a 3.″4 fitting radius, with a PSF determined for each image from 12 isolated stars of about the same aperture magnitude, near the midpoint of the magnitude range for the image. Zero points for the UV magnitudes are determined by averaging *IUE* spectra of seven bright stars in the UIT field, which are also in the Sanduleak catalog (1969), over the UIT filter functions to compute expected magnitudes in the UIT bands (Hill et al. 1993). These *IUE* spectra were used by Fitzpatrick (1985) in his investigations of the 30 Dor extinction curve. The *IUE* spectra were reduced using the standard corrections for the sensitivity degradation of the cameras. Differences between the magnitudes in the UIT bands simulated from *IUE* spectra and the magnitudes computed from the UIT images determine the correc-

[1] Hughes STX, 4400 Forbes Boulevard, Lanham, MD 20706.
[2] Space Telescope Science Institute, Homewood Campus, Baltimore, MD 21218.
[3] University of Virginia, P.O. Box 3818, Charlottesville, VA 22903.
[4] National Radio Astronomy Observatory, operated by Associated Universities Inc. under cooperative agreement with the NSF, Edgemont Rd., Charlottesville, VA 22903.
[5] Laboratory for Astronomy and Solar Physics, NASA/GSFC, Greenbelt, MD 20771.

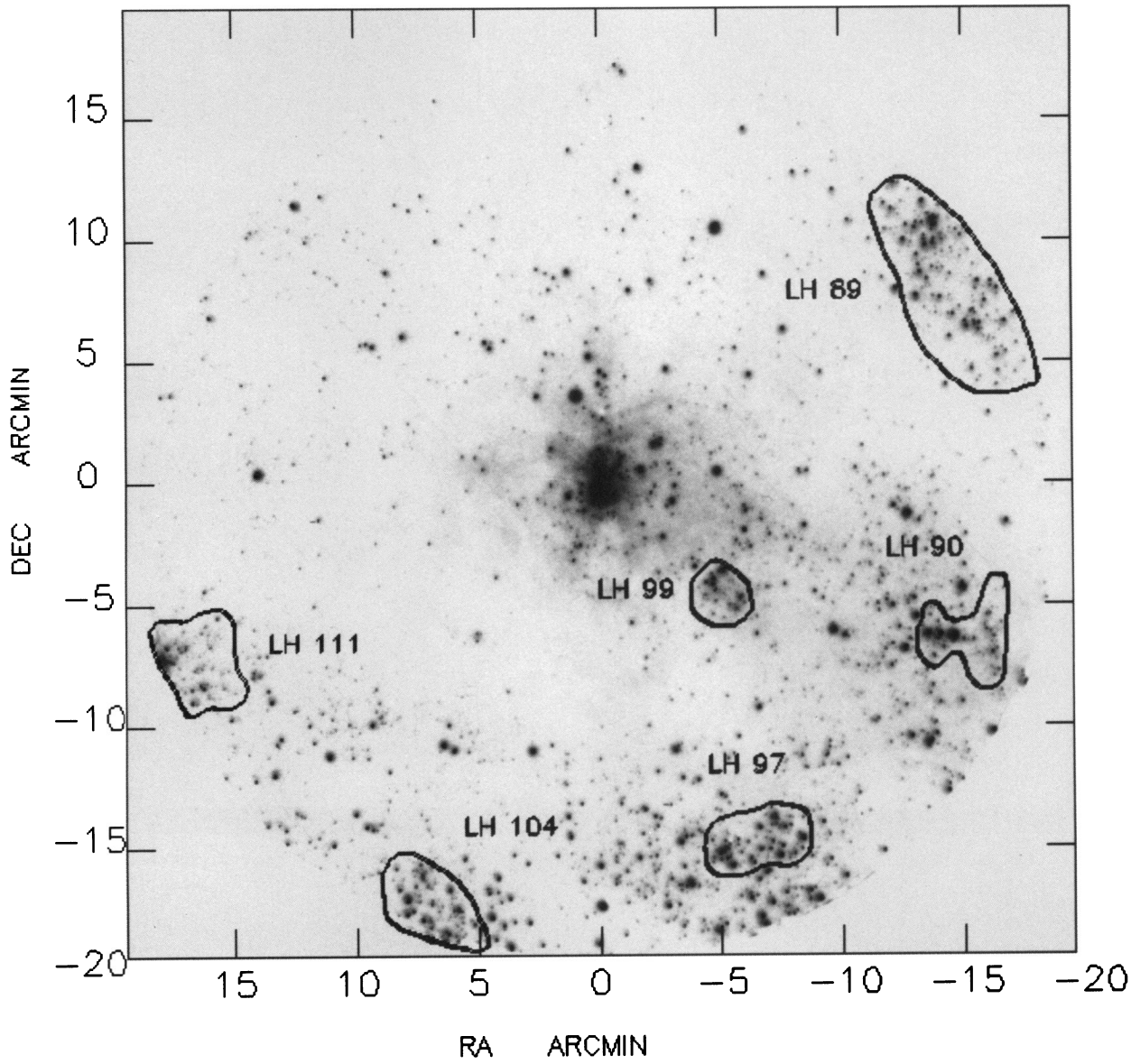


FIG. 1a

FIG. 1.—(*a*) The UIT 472 s A5 band exposure NUV0128, of a 40′ diameter circular field centered near R136. North is up, and east is to the left. Lucke & Hodge (1970) associations LH 89, LH 90, LH 97, LH 99, LH 104, and LH 111 are outlined. (*b*) The UIT 473 s B5 band exposure FUV0137, of a 40′ diameter circular field centered near R136. North is up, and east is to the left.

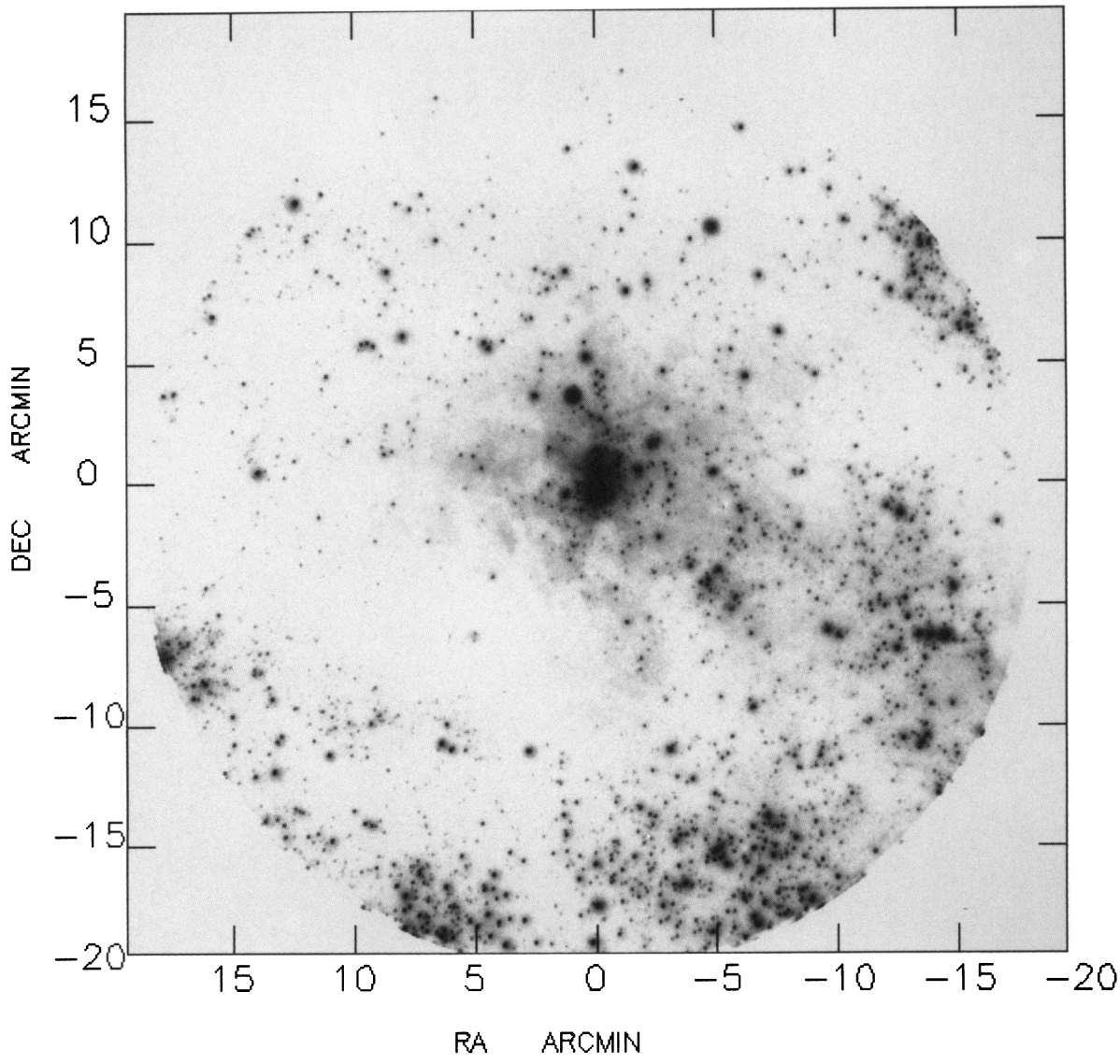


FIG. 1*b*

HILL et al. (see 425, 122)

TABLE 1

UIT IMAGES USED FOR 30 DORADUS STELLAR PHOTOMETRY

| UIT Image | Exposure Time (s) | UIT Bandpass | λ (Å) | Bandwidth (Å) |
|---|---|---|---|---|
| FUV0136..... | 92.9 | B5 | 1615 | 225 |
| FUV0137..... | 473.0 | B5 | 1615 | 225 |
| FUV0138..... | 18.3 | B5 | 1615 | 225 |
| NUV0127..... | 95.0 | A5 | 2558 | 456 |
| NUV0128..... | 472.0 | A5 | 2558 | 456 |
| NUV0129..... | 18.3 | A5 | 2558 | 456 |

tions to the UIT calibration necessary to put the UIT magnitudes on the *IUE* flux scale. The star names and the numbers of the *IUE* spectra are given in Table 2 of Hill et al. (1993). As detailed by Hill et al. (1993), our estimate for the statistical uncertainty in the UIT magnitudes is ~0.10 mag. The uncertainty in the magnitude zero point is ~0.05 mag.

B5 band magnitudes are defined by the relation $m_{162} = -2.5 \times \log(f_{162}) - 21.1$, where $f_{162}$ is the flux in units of ergs (cm$^2$ Å s)$^{-1}$. The B5 magnitudes range from $m_{162} = 9.94$ to $m_{162} = 16.29$, while A5 band magnitudes $m_{256}$, defined by a similar relation, range from $m_{256} = 10.69$ to $m_{256} = 17.11$. Figure 2*a* plots $m_{256}$ histograms in 0.5 mag bins, for stars in LH associations (*solid lines*) and stars outside LH associations (*dashed lines*). Figure 2*b* shows $m_{162}$ histograms for associations (*solid lines*) and the field (*dashed lines*). The association histograms are multiplied by 3.5 to make the association bin populations approximately equal to those in the field. Association membership is assigned on the basis of the association boundaries on the finding charts of Lucke (1972). Field stars are stars which are not within the boundaries of associations. The histogram plots show that the slopes of the UV luminosity functions are shallower in the associations than in the field. The UV magnitudes are presumably incomplete for stars fainter than the histogram peaks at $m_{162} \sim 14.0$ and $m_{256} \sim 15.0$.

Table 2 gives the stellar positions $x$ and $y$ as offsets in arcseconds east and north from the J2000 fiducial position RA = $5^h38^m44^s$ and decl. = $-69°6'32''$ (cols. [2] and [3]), magnitudes $m_{162}$ (col. [4]) and $m_{256}$ (col. [5]), and the LH association number (col. [6]) for those stars in LH associations. The positions are corrected for the effects of image distortions caused by slight magnetic field nonuniformities in the image tubes, to an accuracy ~5″. LH number 0 is assigned to stars not within LH associations. When a star is measured on more than one image in a given UIT band, the average of the individual measurements is adopted. The magnitudes are not corrected for extinction. The fitted mass (in $M_\odot$) and the fitted $E(B-V)$ within 30 Dor, computed as described below, are given in columns (7) and (8). The rms magnitude difference between the observations and the best-fit model is given in column (9). (Only a portion of Table 2 containing five of the brightest stars in each association and the field is included here; the full table is distributed on the AAS CD-ROM Vol. 2.)

Before further analysis, the stellar magnitudes are corrected for foreground Galactic extinction [$E(B-V) = 0.06$] and LMC halo extinction [$E(B-V) = 0.04$], according to the reddening model for the region (Heap et al. 1991). These foreground extinction corrections are 0.82 mag in the B5 band and 0.73 mag in A5, as determined from the Galactic extinction curve (Savage & Mathis 1979) and the general (i.e., non–30 Dor) LMC extinction curve (Fitzpatrick 1985). Further extinction is assumed to take place in 30 Dor, following the 30 Dor reddening curve of Fitzpatrick (1985).

## 3. DETERMINATION OF MASSES AND EXTINCTIONS

Figure 3 shows the observed UIT color-magnitude diagram (CMD), with age 3, 4, 5, and 6 Myr isochrones overplotted, for $E(B-V)$ equal to the average of the fitted values for the individual stars, computed as described below. Initial mass values are indicated for several points on the isochrone. Initial stellar masses and extinctions within the 30 Dor region are deter-

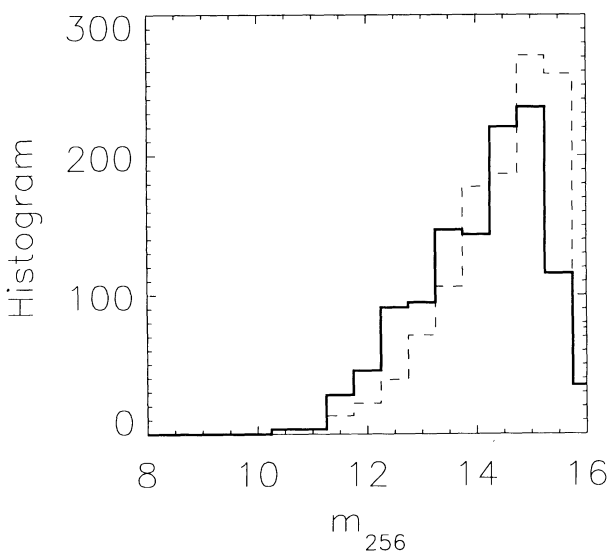


FIG. 2*a*

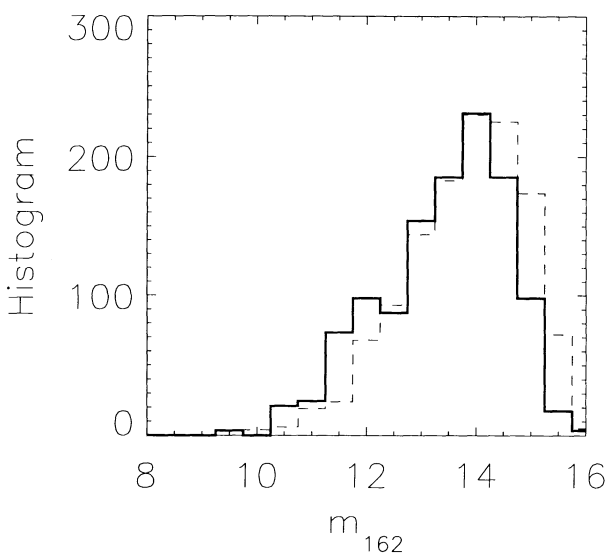


FIG. 2*b*

FIG. 2.—(*a*) Histograms of the stellar magnitudes measured in the near-UV A5 band for stars in LH associations (*solid line*) and field stars (*dashed line*). The histogram for association stars has been multiplied by 3.5. (*b*) Histograms of the stellar magnitudes measured in the far-UV B5 band for stars in LH associations (*solid line*) and field stars (*dashed line*). The histogram for association stars has been multiplied by 3.5.

TABLE 2

OBSERVED AND FITTED STELLAR DATA

| ind | x | y | $m_{162}$ | $m_{256}$ | LH | mass | E(B-V) | rms |
|---|---|---|---|---|---|---|---|---|
| 967 | -756.1 | 650.2 | 10.73 | 11.73 | 89 | 34.0 | 0.11 | 0.01 |
| 935 | -810.3 | 637.0 | 10.82 | 11.86 | 89 | 32.0 | 0.10 | 0.01 |
| 811 | -906.1 | 432.2 | 11.24 | 11.89 | 89 | 43.0 | 0.23 | 0.03 |
| 970 | -785.5 | 678.9 | 11.93 | 12.06 | 89 | 53.0 | 0.35 | 0.04 |
| 867 | -840.4 | 507.1 | 11.57 | 12.24 | 89 | 38.0 | 0.23 | 0.04 |
| 112 | -955.7 | -367.1 | 11.71 | 12.45 | 90 | 34.0 | 0.21 | 0.02 |
| 232 | -837.5 | -350.7 | 12.03 | 12.58 | 90 | 40.0 | 0.29 | 0.03 |
| 204 | -885.4 | -330.0 | 12.27 | 12.65 | 90 | 41.0 | 0.32 | 0.03 |
| 230 | -814.8 | -373.4 | 11.94 | 12.87 | 90 | 26.0 | 0.15 | 0.02 |
| 263 | -823.2 | -329.2 | 12.56 | 12.89 | 90 | 41.0 | 0.35 | 0.01 |
| 193 | -386.6 | -792.8 | 11.03 | 11.74 | 97 | 42.0 | 0.20 | 0.02 |
| 219 | -288.3 | -854.3 | 11.31 | 11.95 | 97 | 42.0 | 0.23 | 0.01 |
| 143 | -447.6 | -790.9 | 11.24 | 12.10 | 97 | 34.0 | 0.16 | 0.01 |
| 124 | -371.6 | -878.3 | 11.70 | 12.12 | 97 | 44.0 | 0.28 | 0.03 |
| 142 | -386.9 | -845.3 | 10.98 | 12.22 | 97 | 24.0 | 0.03 | 0.01 |
| 779 | -305.2 | -156.3 | 10.57 | 11.15 | 99 | 50.0 | 0.20 | 0.01 |
| 781 | -295.6 | -160.7 | 12.05 | 12.20 | 99 | 50.0 | 0.35 | 0.03 |
| 699 | -344.9 | -224.8 | 11.68 | 12.38 | 99 | 36.0 | 0.22 | 0.03 |
| 758 | -284.7 | -205.1 | 12.07 | 12.58 | 99 | 41.0 | 0.30 | 0.04 |
| 739 | -285.2 | -232.5 | 12.91 | 13.50 | 99 | 28.0 | 0.27 | 0.00 |
| 685 | 472.1 | -960.4 | 9.94 | 10.69 | 104 | 49.0 | 0.13 | 0.02 |
| 663 | 473.9 | -994.6 | 11.16 | 11.70 | 104 | 46.0 | 0.24 | 0.02 |
| 720 | 493.6 | -935.1 | 11.83 | 12.55 | 104 | 33.0 | 0.21 | 0.01 |
| 662 | 461.0 | -986.4 | 11.91 | 12.60 | 104 | 34.0 | 0.23 | 0.02 |
| 512 | 292.2 | -1033.4 | 11.94 | 12.65 | 104 | 32.0 | 0.21 | 0.03 |
| 1118 | 961.6 | -433.9 | 10.98 | 12.22 | 111 | 24.0 | 0.03 | 0.01 |
| 1107 | 990.9 | -468.9 | 11.53 | 12.61 | 111 | 23.0 | 0.07 | 0.02 |
| 1175 | 929.1 | -262.6 | 12.66 | 12.97 | 111 | 41.0 | 0.36 | 0.00 |
| 1130 | 991.8 | -435.7 | 12.12 | 13.03 | 111 | 23.0 | 0.13 | 0.03 |
| 1126 | 969.5 | -425.2 | 12.65 | 13.36 | 111 | 26.0 | 0.22 | 0.02 |
| 32 | -387.8 | -1013.3 | 10.19 | 11.20 | 0 | 41.0 | 0.11 | 0.05 |
| 40 | -414.2 | -980.0 | 10.36 | 11.30 | 0 | 41.0 | 0.13 | 0.02 |
| 1205 | 67.9 | 576.7 | 10.72 | 11.37 | 0 | 47.0 | 0.20 | 0.02 |
| 983 | -456.2 | 428.0 | 10.77 | 11.42 | 0 | 46.0 | 0.20 | 0.01 |
| 197 | -163.6 | -985.5 | 11.06 | 11.58 | 0 | 48.0 | 0.24 | 0.01 |

NOTE.—Table 2 is published in its entirety in computer-readable form in the AAS CD-ROM Series, Vol. 2.

mined using a least-squares technique. The evolutionary models of Schaerer et al. (1993) with LMC metallicity (log $z = 0.008$), which include the effects of mass loss and convective overshoot, are interpolated to a mass grid ranging from 5 to 54 $M_\odot$ in intervals of 1 $M_\odot$, for assumed ages equal to 3, 4, 5, and 6 Myr. In order to fit masses from stellar models, it is necessary to know, or assume, the age. The feasibility of determining the stellar mass and the extinction from the measured magnitudes is demonstrated by the angle which the dereddening arrow in Figure 3 makes with the plotted isochrones. The orientation of the arrow is determined by the reddening curve adopted. In order to simultaneously estimate stellar reddening and mass it is necessary that the dereddening arrow not be parallel to the isochrone.

Heap et al. (1993) estimate the age of R136a at 3 Myr from the presence of bright early-type W-R stars. The associations treated here most likely have ages greater than 3 Myr, but less than 6 Myr. The lower limit follows from the absence of stars bright enough to be W-R stars of initial mass $\sim 100\ M_\odot$. The upper limit follows from the presence in Figure 3 of observed stars brighter than the most massive star on the 6 Myr isochrone. We assumed the age of the association stars to be 4 Myr.

The value of the assumed age is important for stars whose main-sequence lifetimes are comparable to the assumed age or less. Stars whose fitted masses are $\sim 35\ M_\odot$, assuming age 4 Myr, will have fitted masses equal to $\sim 40\ M_\odot$ if the age is assumed to be 3 Myr and $\sim 30\ M_\odot$ for age 5 Myr. The dependence of the fitted mass on the assumed age (in the range 3–6 Myr) decreases for lower masses. The masses in Table 2 for stars in associations were computed assuming age 4 Myr. The masses of stars not in associations were computed assuming an age equal to either 4 Myr or half the main-sequence stellar lifetime from the Schaerer et al. (1993), models, whichever is larger. Lifetimes in Myr are given in Table 3 for massive stars, as estimated from the models of Schaerer et al. (1993).

Simulated UIT $m_{162}$ and $m_{256}$ magnitudes are computed for the models by integrating Kurucz (1992) model atmospheres with the appropriate effective temperature, metallicity, and surface gravity over the UIT filter functions. For each of the 50 mass points in the grid, B5 and A5 magnitudes are computed for 40 values of additional local $E(B-V)$, ranging from 0.00 to

TABLE 3

STELLAR LIFETIMES FROM MODELS OF SHAERER ET AL.

| Mass ($M_\odot$) | Lifetime (Myr) |
|---|---|
| 10 | 24 |
| 12 | 18 |
| 15 | 13 |
| 20 | 9 |
| 25 | 7.5 |
| 40 | 5 |
| 60 | 4 |
| 85 | 3 |

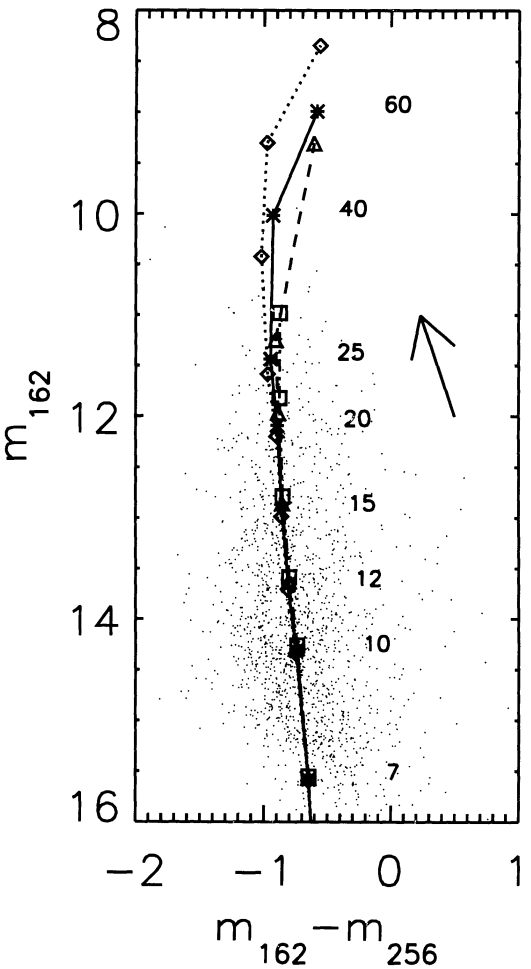


FIG. 3.—Observed $m_{162} - m_{256}$ vs. $m_{162}$ color-magnitude diagram. The 3, 4, 5, and 6 Myr isochrones from the evolutionary models of Schaerer et al. (1993) with LMC metallicity are shown as solid lines, with plot symbol diamond (*dotted line*), asterisk (*solid line*), triangle (*dashed line*), and box (*dot-dashed line*), respectively, for local $E(B-V)$ equal to 0.182, the average of the fitted values. The dereddening arrow implied by the 30 Dor reddening curve of Fitzpatrick (1985) is shown.

0.39 in intervals of 0.01. The reddened model UV magnitudes are computed using the Fitzpatrick (1985) 30 Dor reddening curve. The best-fit mass and reddening are computed for each star by determining which of the grid of 2000 mass-reddening models has the minimum mean-square deviation from the observed $m_{162}$, $m_{256}$ magnitude pair. The distance modulus is assumed to be 18.57, as previously adopted by Heap et al. (1991) and Hill et al. (1993). The uncertainty in the best-fit mass from photometric errors is estimated at $\sim$0.25 of the fitted mass.

## 4. INITIAL MASS FUNCTIONS (IMFS)

The LH association IMF is computed from the fitted masses for the sample of 311 stars in LH associations with rms fit errors less than 0.2 mag. The field star IMF is computed from the sample of 1154 stars with fit errors less than 0.2 mag which are not in associations. The IMF $F[\log(m)]$ is characterized by the parameter $\Gamma = \partial \log F[\log(m)]/\partial \log(m)$. The mass function computed for stars in associations has slope $\Gamma = -1.08 \pm 0.2$ and is plotted in Figure 4*a*. The IMF for stars not in LH associations is steeper than the association star mass function, with slope $\Gamma = -1.74 \pm 0.3$. In the Galaxy, most young cluster IMFs are also flatter than the field star IMF (Scalo 1986). The large difference between the present-day mass functions of the associations and the field is illustrated by the fact that 17% of the association stars we measure have fitted masses greater than 30 $M_\odot$, while only 6.8% of the field stars have fitted masses greater than this limit.

The field star IMF, plotted in Figure 4*b*, is computed from the present-day mass function, by dividing the mass histogram by the appropriate stellar lifetime as a function of stellar mass (Salpeter 1955; Scalo 1986). This correction acts to flatten the computed IMF compared with the observed mass function, since the lower mass stars have longer lifetimes. Salpeter (1955) estimated the slope of the IMF in the solar neighborhood at $\Gamma = -1.35$, while Scalo's (1986) estimated Galactic IMF slope for massive stars of $-1.7 \pm 0.5$ is nearly equal to our estimate of the field star IMF slope. Garmany, Conti, & Chiosi (1982) determine the slope of the IMF for massive stars in the Galaxy at $-1.6$.

To test the likely effect of photometric errors on the IMF slopes, we add Gaussian-distributed random variables with mean value 0 and standard deviation 0.1 to the measured magnitudes $m_{162}$ and $m_{249}$, and repeat the determination of masses and IMF slopes. The IMF slopes obtained after following this process are $-1.17$ for the associations and $-1.71$ for the field. These estimates differ from the original slopes by much less than the error estimates in the slopes of 0.2 and 0.3 computed from the counting statistics of the binned masses. Given the estimated uncertainties in the slopes, we conclude that the difference between them, 0.66, is significant, and equal to 1.8 times its estimated uncertainty.

No correction has been made for binaries or incompleteness. In the extreme case of a binary with equal mass components, the individual star masses would be about 0.8 times the mass inferred for the system, when treated as a single star. The slope of the mass function would be affected significantly only if the percentage of "stars" which are actually equal mass binaries varies strongly with mass, for masses greater than 10 $M_\odot$. Our result that the IMF for the associations has a shallower slope than the field IMF is unaffected by binaries, unless the frequency of binaries differs greatly between the associations and the field. Secondaries of later spectral type and lower mass than the primary make a negligible contribution to the flux in our UV bands (Fanelli 1994).

We conclude that the IMF for massive stars in the 30 Dor region more than 5′ from R136 is more heavily weighted toward massive stars in the Lucke & Hodge associations than in the field. We also conclude that the field star IMF slope is slightly steeper than Salpeter's solar neighborhood value, $\Gamma = -1.35$ (Salpeter 1955), but nearly equal to Scalo's (1986) IMF slope, $\Gamma = -1.7 \pm 0.5$. OB associations are apparently regions in which the star formation rate is not merely higher but is more heavily weighted toward massive stars than in the field.

Table 4 gives the average $E(B-V)$ inferred for the stars in each LH association and the field (association 0), together with the standard deviation of the fit values in each case. $E(B-V)$ values determined by Lucke (1974) (which include the foreground reddening) are also given. After subtracting the foreground reddening [$E(B-V) = 0.10$], the $E(B-V)$ values given by Lucke (1974) are less than 1 standard deviation from the mean $E(B-V)$ we determine. The fact that the $E(B-V)$ values

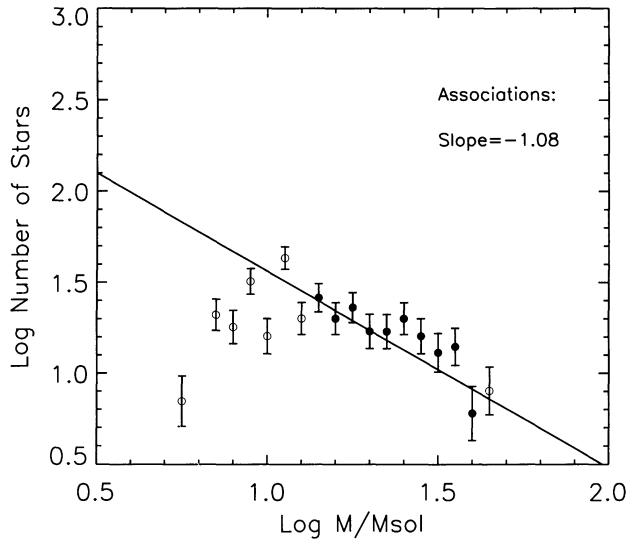


FIG. 4a

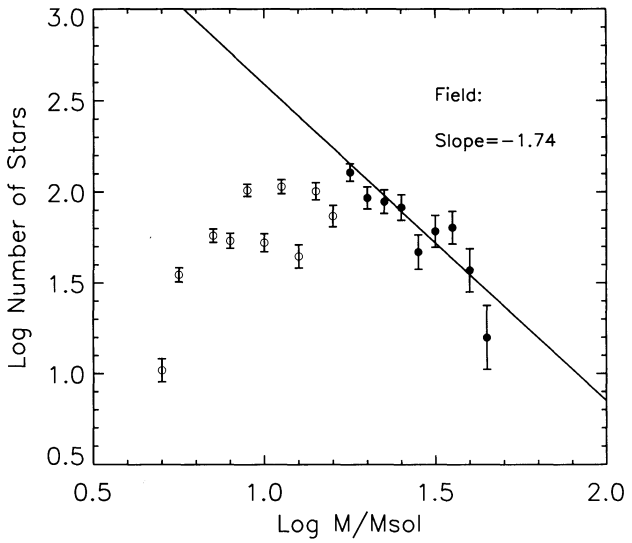


FIG. 4b

FIG. 4.—(*a*) IMF for the stars in LH associations. The points used in the fit to determine Γ are plotted as solid circles with error bars. The points not used in the fit because of incompleteness are plotted as open circles with error bars. (*b*) IMF for the stars not in LH associations. The points used in the fit to determine Γ are plotted as solid circles with error bars. The points not used in the fit because of incompleteness are plotted as open circles with error bars.

TABLE 4

AVERAGE FIT $E(B-V)$ OF ASSOCIATIONS

| Association | Average fit $E(B-V)$ | Standard Deviation | $E(B-V)$ from Lucke |
|---|---|---|---|
| 89..... | 0.21 | 0.10 | 0.37 |
| 90..... | 0.27 | 0.11 | 0.26 |
| 97..... | 0.13 | 0.10 | 0.23 |
| 99..... | 0.23 | 0.11 | ... |
| 104..... | 0.13 | 0.10 | 0.23 |
| 111..... | 0.21 | 0.12 | 0.26 |
| 0..... | 0.16 | 0.12 | ... |

we obtain from UV photometry are consistent (within the observational scatter) with the values obtained by Lucke (1974) from optical photographic photometry means that the UIT photometry is consistent with the Fitzpatrick (1985) 30 Dor extinction curve.

## 5. SUMMARY

UV magnitudes of 1563 stars, in LH associations and the field, are determined from UIT images in two bands of the 30 Dor region of the LMC. The model atmospheres of Kurucz (1992) and the evolutionary models of Schaerer et al. (1993) are used to estimate stellar masses, assuming the extinction follows the 30 Dor extinction curve of Fitzpatrick (1985). The age of the association stars is assumed to be 4 Myr, while the age of the field stars is assumed to be half the hydrogen burning stellar lifetime, or 4 Myr, whichever is larger. IMFs computed for the massive stars have slope −1.08 in the associations and −1.74 in the field, similar to the IMF in the Galaxy (Scalo 1986; Garmany et al. 1982). The shallower slope of the IMF in the Lucke & Hodge associations suggests not only that the star formation rate is locally higher there, but also that conditions are especially favorable for the formation of massive stars.

We gratefully acknowledge the innumerable contributions made by the many people involved in the Astro-1 mission, including the many officials at NASA Headquarters whose support brought it through a long and difficult gestation period.

Funding for the UIT project has been through the Spacelab Office at NASA Headquarters under project number 440-51. R. W. O. acknowledges NASA support of portions of this research through grants NAG 5-700 and NAGW-2596 to the University of Virginia.

## REFERENCES

Campbell, B., et al. 1992, AJ, 104, 1721
Cheng, K.-P., et al. 1992, ApJ, 395, L29
Fanelli, M. N. 1994, in preparation
Fitzpatrick, E. L. 1985, ApJ, 299, 219
Garmany, C. D., Conti, P. S., & Chiosi, C. 1982, ApJ, 263, 777
Heap, S. R., et al. 1991, ApJ, 377, L29
Heap, S. R., Ebbets, D., & Malamuth, E. 1993, in Science with the *Hubble Space Telescope*, ed. P. Benvenuti & E. Schreier (Garching: ESO), 347
Hill, J. K., et al. 1993, ApJ, 413, 604
Kurucz, R. L. 1992, in The Stellar Populations of Galaxies, ed. B. Barbuy & A. Renzini (Dordrecht: Kluwer), 225
Lasker, B. M., Sturch, C. R., McLean, B. J., Russell, J. L., Jenker, H., & Shara, M. M. 1990, AJ, 99, 2019
Lucke, P. B. 1972, Ph.D. thesis, Univ. Washington
———. 1974, ApJS, 28, 73
Lucke, P. B., & Hodge, P. W. 1970, AJ, 75, 171
Malamuth, E., & Heap, S. R. 1993, AJ, in press
Parker, J. Wm. 1992, Ph.D. thesis, Univ. of Colorado
Salpeter, E. E. 1955, ApJ, 121, 161
Sanduleak, N. 1969, Cerro Tololo Inter-American Obs. Contrib. No. 89
Savage, B. D., & Mathis, J. S. 1979, ARA&A, 17, 73
Scalo, J. M. 1986, Fund. Cosmic Phys., 11, 1
Schaerer, D., Meynet, G., Maeder, A., & Schaller, G. 1993, A&AS, 98, 523
Schild, H., & Testor, G. 1992, A&AS, 92, 729
Stecher, T. P., et al. 1992, ApJ, 395, L1
Stetson, P. B. 1987, PASP, 99, 101